

Image Quality in Digital Mammography: Image Acquisition

Mark B. Williams, PhD^a, Martin J. Yaffe, PhD^b, Andrew D.A. Maidment, PhD^c,
Melissa C. Martin, MS^d, J. Anthony Seibert, PhD^e, Etta D. Pisano, MD^f

This paper on digital mammography image acquisition is 1 of 3 papers written as part of an intersociety effort to establish image quality standards for digital mammography. The information included in this paper is intended to support the development of an ACR guideline on image quality for digital mammography. The topics of the other 2 papers are digital mammography image display and digital mammography image storage, transmission, and retrieval. The societies represented in compiling this document were the Radiological Society of North America, the ACR, the American Association of Physicists in Medicine, and the Society for Computer Applications in Radiology. These papers describe in detail what is known to improve image quality for digital mammography and make recommendations about how digital mammography should be performed to optimize the visualization of breast cancers. Through the publication of these papers, the ACR is seeking input from industry, radiologists, and other interested parties on their contents so that the final ACR guideline for digital mammography will represent the consensus of the broader community interested in these topics.

Key Words: Digital mammography, image acquisition, image quality

J Am Coll Radiol 2006;3:589-608. Copyright © 2006 American College of Radiology

INTRODUCTION AND OVERVIEW OF MAMMOGRAPHIC IMAGE QUALITY

Theoretical Quality of the Acquired Radiographic Image

Task-Dependent Image Quality. The analysis of image quality has meaning only in the context of a particular imaging task [1]. For example, a mammographic imaging system must permit the detection and characterization of small microcalcifications (requiring very high spatial resolution), whereas a positron emission tomographic scanner must be able to identify subtle differences in radiopharmaceutical concentration (requiring high contrast transfer ability but at lower spatial resolution). Therefore, to be useful in assessing image quality, any figures of merit must take into account the properties of the specific imaging task. Accordingly, this paper on

digital mammography image acquisition, together with its companion papers on digital mammography display and digital mammography storage, transmission, and retrieval, was developed with reference to the specific imaging tasks required by mammography, using the information available in the peer-reviewed medical literature.

Ultimately, image quality is affected by both image acquisition and image display. Thus, particularly in digital systems, in which these functions are clearly separable, the analysis of image quality can be performed in 2 stages. In the first stage, the direct laboratory measurement of the physical properties of an image acquisition system itself (ie, its spatial resolution, noise, and sensitivity) can be used to predict system performance before an image is presented to an observer. The observer can be a human or a mathematical construct, one example of which is the "ideal observer model." The ideal observer makes optimal use of both the signal and the noise contained in an acquired image, thus representing a quantitative measurement of the highest possible performance level. The measured physical properties are combined mathematically with a description of the particular imaging task to yield a figure of merit (such as the ideal observer signal-to-noise ratio [SNR_I]) that indicates how well positive (abnormal) and negative (normal) results can be differentiated [1]. The primary drawbacks to the ideal observer analysis are that (1) it is difficult to specify complex imaging tasks, including, for example, realistic

^aUniversity of Virginia, Charlottesville, Va.

^bSunnybrook & Women's College Health Sciences Centre, University of Toronto, Toronto, Ont, Canada.

^cHospital of the University of Pennsylvania, Philadelphia, Pa.

^dTherapy Physics Inc., Bellflower, Calif.

^eUniversity of California, Davis, Medical Center, Sacramento, Calif.

^fUniversity of North Carolina at Chapel Hill, Chapel Hill, NC.

Corresponding author and reprints: Mark B. Williams, PhD, University of Virginia, Department of Radiology, PO Box 801339, Charlottesville, VA 22908-1339; e-mail: mbwilliams@virginia.edu.

background structure; (2) the results may not represent the performance of real human observers; and (3) accurate measurements of the physical properties of an image acquisition system are often difficult to make.

In the second stage of analysis, images are presented to human observers in the context of a receiver operating characteristic (ROC) study, in which diagnostic sensitivity and specificity can be determined over a range of levels of observer aggressiveness (ie, how willing they are to accept false-positive results to avoid false-negative results) [2,3]. The major strengths of ROC studies are that they include all aspects of an imaging system, including the human observer, and they use a realistic and meaningful imaging task. The main drawbacks of ROC studies using human observers are that they are extremely resource and time consuming.

A more efficient approach, therefore, is to first analyze an acquisition system using measured physical performance metrics and a mathematical observer model and to then use the results to identify promising sets of system configuration parameters to be tested in human observer performance studies.

Mammography as an Example of the Decision-Making Paradigm. The presence or absence of a lesion in a mammogram is an example of a 2-class detection process. Simply put, a radiologist must make a decision as to whether a suspicious lesion is present (ie, the case is positive) or not (ie, the case is negative). According to statistical decision theory, each image can be considered to come from either a set of truly positive cases or a set of truly negative cases. The ability of an imaging system to differentiate between data taken from the 2 populations can be quantified by examining the results produced by a decision maker who, when given data from the system (ie, an image), is asked to decide from which of the 2 populations the data arose. The decision maker uses some type of decision variable based on 1 or more image features (eg, the presence of specific patterns in the image characteristic of masses, calcifications, or architectural distortion) to classify each image. If decision variable values are generated for each of a large number of images, a histogram of the resulting values forms 2 distributions, as shown in Figure 1, 1 corresponding to the normal (negative) population and 1 to the abnormal (positive) population. The horizontal axis represents the variable or variables used to make the decision. As shown in the figure, these distributions typically have some overlap. Case-to-case variations in lesion shape and size, noise introduced during the image acquisition process, and interobserver and intraobserver variability all serve to broaden the negative and positive distributions along the decision axis and result in overlap of the 2. Each observer must establish a decision threshold (shown as a vertical

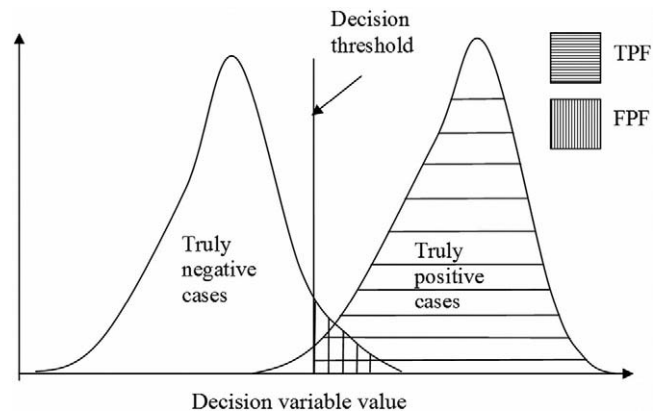


Fig 1. Schematic diagram showing the overlap between the decision variable histograms obtained by imaging cases drawn from both truly positive and truly negative populations. The fraction of truly negative cases with decision variable values greater than the decision threshold is the false-positive fraction (FPF). The fraction of truly positive cases with decision variable values greater than the decision threshold is the true-positive fraction (TPF).

line in Figure 1), below which an image is considered negative and above which it is considered positive. The location of this threshold along the range of possible values of the decision variable(s), along with the widths and separations of the 2 populations, determines the false-positive fraction and true-positive fraction. As shown in the figure, the false-positive fraction and true-positive fraction are the fractions of truly negative and truly positive cases, respectively, determined to be positive. Measurement of the false-positive fraction and true-positive fraction as the decision threshold is systematically varied as the basis of the ROC methodology, which is described in more detail later in this paper.

Given the distributions of the decision variable for the 2 hypotheses (Figure 1), it is possible to define an effective SNR as figure of merit describing the ability of the combined imaging system and decision maker to differentiate between negative and positive cases. If the signal is defined as the difference between the means of the distributions and the noise is defined as the average of their standard deviations, then the square of the SNR is

$$\text{SNR}^2 = (\langle L \rangle_2 - \langle L \rangle_1)^2 / [1/2(\sigma_1^2 + \sigma_2^2)],$$

where L is the decision variable, $\langle \rangle$ denotes averaging, σ is the standard deviation of a distribution, and the subscripts 1 and 2 refer to normal and abnormal, respectively. This definition of the SNR is general and holds for all types of decision makers (observers) and all assumptions about the data (eg, how well the lesion shape and nature of the background are known). However, for some specific types of observers and specific assumptions

about the nature of the data and image noise, the SNR can be rewritten in terms of measurable quantities. One of the most useful observer types is the ideal Bayesian observer. The ideal observer SNR, SNR_I , is a direct measure of the degree of overlap between the 2 probability distributions in the circumstance in which they have not been broadened by variability introduced during the decision-making process (ie, reader variability). The measurement of SNR_I is thus the first stage of the quantitative assessment of image quality, namely, the assessment of the acquired data.

The Ideal Observer Formalism for Assessment of the Quality of the Acquired Data. The ideal observer calculates the likelihood (probability), given the image data, that a patient is truly a member of the negative population and, similarly, the likelihood that she is truly a member of the positive population. The ratio of these 2 probabilities (ie, the likelihood ratio) is used as a decision variable. A given image is considered normal if the decision variable is less than a predetermined threshold value and abnormal if it is greater. The “ideal” aspect of this observer is that it decides in favor of the hypothesis that minimizes the probability of making an incorrect judgment [1]. The ideal observer is able to first identify spatial correlations in the image noise (eg, to recognize detector artifact noise in the digital mammogram) and to effectively remove it (in other words, to remove the spatial correlation or whiten the noise). In situations in which the signal shape (ie, lesion shape) is known, the ideal observer then uses the known shape as a filter to identify areas in the image that most closely match the filter. This strategy, therefore, is known as the prewhitened matched filter. It can be shown [1,4] that for linear, shift-invariant imaging systems, the square of the ideal observer SNR can be written as

$$\text{SNR}_I^2 = K^2 \int |\Delta f(\mathbf{v})|^2 \text{MTF}^2(\mathbf{v}) / W_n(\mathbf{v}) d\mathbf{v},$$

where the quantities $\Delta f(\mathbf{v})$, $\text{MTF}(\mathbf{v})$, and $W_n(\mathbf{v})$ are functions of the spatial frequency variable \mathbf{v} . For 2-D images, \mathbf{v} is actually 2-D and can be considered in terms of its components v_x and v_y . $\Delta f(\mathbf{v})$ is the Fourier transform of the difference in signals under the 2 competing hypotheses (eg, lesion present vs lesion absent for the problem of the detection of disease or type 1 lesion present vs type 2 lesion present for the problem of characterization), $\text{MTF}(\mathbf{v})$ is the modulation transfer function of the image acquisition system, and $W_n(\mathbf{v})$ is the Wiener, or noise power, spectrum. The constant K is a scaling factor relating units at the output of the imaging system (eg, analog-to-digital units or optical density) to units at its input (x-ray photons per unit area).

The MTF describes the spatial resolution of the imaging system in terms of its ability to transfer signal from its input to output as a function of the spatial frequency of

the signal. $W_n(\mathbf{v})$ is the Fourier decomposition of the image variance and describes the spatial frequency dependence of the total noise, including system noise and x-ray photon noise. The quantities K , $\text{MTF}(\mathbf{v})$, and $W_n(\mathbf{v})$ can be determined from laboratory measurements made under a particular set of operating conditions (eg, particular x-ray beam quality and exposure settings) using simple phantoms [5,6]. They are often combined to form a quantity called the noise equivalent quanta (NEQ):

$$\text{NEQ}(\mathbf{v}) = K^2 \text{MTF}^2(\mathbf{v}) / W_n(\mathbf{v}).$$

The NEQ is a direct measurement of the quality of the acquired image and has units of input quanta per unit area. It can be interpreted as the number of quanta per area at the input of a perfect imaging system that would be necessary to achieve the measured image quality.

The quantity $\Delta f(\mathbf{v})$ depends on the particular imaging task (eg, mass or microcalcification) and ensures that the derived SNR_I is task specific. Thus, SNR_I can also be written

$$\text{SNR}_I^2 = \int |\Delta f(\mathbf{v})|^2 \text{NEQ}(\mathbf{v}) d\mathbf{v}.$$

In digital mammography, the specific imaging task is accurate depiction of mass morphology, microcalcification morphology, architectural distortion, and left-right breast asymmetry, all in the presence of normal structure background [7]. So, for example, $\Delta f(\mathbf{v})$ could be the Fourier transform of the spatial distribution of a mass (ie, the 2 hypotheses are that a mass is or is not present). The important physical performance characteristics for high-quality mammographic image acquisition are high MTF, that the system itself not contribute appreciably to W_n (ie, that the image noise is primarily x-ray quantum noise), a large dynamic range, and good contrast transfer. The latter property refers to the maximization of the subject contrast (the contrast in x-ray fluence incident at various points on the detector surface, produced by differences in attenuation along paths through the breast) by the use of optimal x-ray techniques, combined with high detector absorption efficiency (quantum detection efficiency).

ROC Evaluation. The ROC curve is a graph describing, for a particular interpreter or averaged over multiple interpreters, their sensitivity in detecting breast cancer compared with $1 - \text{specificity}$ (ie, their true-positive fraction vs their false-positive fraction). Thus, an important advantage of the ROC method is that the outcome variables are absolutely appropriate, providing an assessment of the accuracy of determining whether or not cancer is present. Two hypothetical ROC curves are illustrated in Figure 2. All ROC curves contain the points (0,0) (perfect specificity but zero sensitivity by calling all

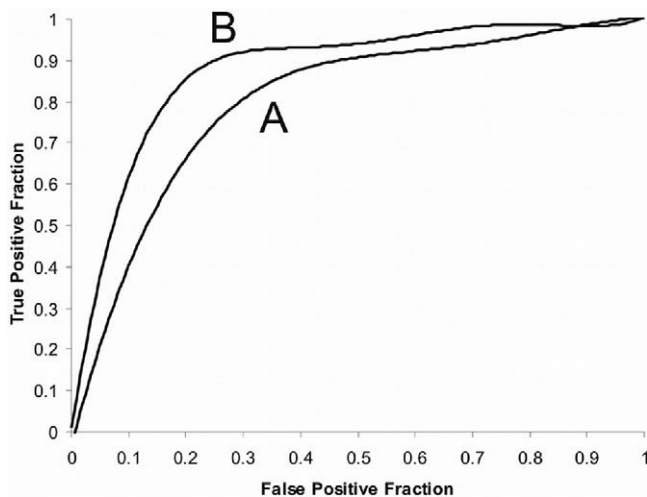


Fig 2. Hypothetical receiver operating characteristic curves. For any given sensitivity (true-positive fraction), the curve gives the false-positive fraction that would result for that system (averaged over many readers). Moving along a curve indicates reading with different levels of aggressiveness. Curve B represents a better system than curve A because at any false-positive fraction, the sensitivity is higher than for curve A.

examinations negative) and (1,1) (perfect sensitivity but zero specificity by calling all examinations positive). In between, the curve reflects the trade-off between sensitivity and specificity as an observer changes the level of aggressiveness or conservatism used in interpreting the image. Therefore, the path along a particular ROC curve indicates changing the approach taken in reading an image rather than the quality of the images or the readers.

In Figure 2, curve B is higher than curve A, implying that at any chosen level of aggressiveness, a reader (or an imaging system) represented by this curve performs better than that represented by curve A. For a study to be meaningful, it would also be important that the images reflect the relevant target population in terms of breast characteristics and the prevalence of disease and that, through biopsy and follow-up, the truth be known regarding the disease status for each examination.

In an ROC study, the entire diagnostic imaging chain is evaluated, including the acquisition components, display components, and human observer. Thus, such a study represents the ideal means of assessing mammographic image quality. The main drawbacks of observer performance studies are that they are extremely resource and time consuming. For example, the reading image set must contain an adequate number of cases to achieve an acceptable level of confidence in the result. If small differences between ROC curves are to be investigated, the number of images required to provide statistical signifi-

cance can be very large. If a technology (rather than the performance of a particular reader) is being evaluated, the study will have to be performed with multiple readers and possibly with multiple readings per reader [8]. This imposes an enormous time and labor commitment on the readers, normally busy radiologists. The problem becomes especially difficult when it is desired to evaluate mammography in the context of screening. In screening mammography, the number of cancers may only be 3 to 5 per 1,000 examinations. For a meaningful evaluation, the reading set must then contain a relatively small fraction of cancer cases. Furthermore, because testing more than a single configuration of the imaging system or systems requires a separate study, performing such testing at regular intervals can cause the size of the image set to be increased to the point at which the task of reading is at best onerous and at worst impractical.

Mammographic Image Quality

Regardless of whether an image is obtained in analog or digital form, breast cancer is detected on the basis of 4 types of signs on the mammogram [7]:

- (1) the characteristic morphology of a tumor or mass,
- (2) the shape and spatial configuration of mineral deposits called microcalcifications,
- (3) distortion of the normal architecture of the breast tissue, and
- (4) asymmetry between images of the left and right breast.

The primary goal of mammography is to accurately visualize these signs if they exist. At the same time, it is important that these signs not be falsely identified if they are not actually present in the breast. To achieve these goals, it is necessary that the images be of high quality. A high-quality image is one that provides high sensitivity in detecting breast cancer and, at the same time, high specificity to identify a normal breast. Two aspects of image quality can be distinguished: technical and clinical. It is relatively easy to make technical measurements describing the above attributes and reasonable to infer a connection between these technical measures and clinical image quality [9].

THE ACQUISITION PROCESS IN DIGITAL MAMMOGRAPHY

The digital mammography acquisition process is defined as all steps in image formation up to the point at which a digital image is sent to a display device for viewing. This includes patient positioning; the generation and shaping of the x-ray beam (both spatially and from the standpoint of the energy spectrum); the interaction between the beam and the compression paddle, breast, and detector;

the digitization of the detector output; and acquisition-related digital image processing. Acquisition processing compensates for specific, consistent imperfections in the acquisition process through techniques such as removing offsets from detector dark current and correcting for spatial variations in detector sensitivity or in x-ray beam intensity. Some manufacturers may also perform compensation for a decrease in the MTF at this point. Subsequent image processing of the resulting “for-processing” (or raw) image from the acquisition device provides specialized image enhancement techniques to produce a “for-presentation” image for interpretation by a radiologist and for image archiving.

A digital detector has a faithful response to the intensity of incident x-rays over a very wide range. It can be designed to efficiently absorb x-rays, produce an electronic signal, digitize the signal, and store the results in computer memory. The output image is saved as a 2-D matrix in which each element represents the x-ray transmission corresponding to a particular path through the breast.

At present, there are several designs of digital mammography systems either being used clinically or being evaluated pending regulatory approval. Four designs are shown schematically in Figure 3. In all of these except photostimulated storage phosphor (PSP) systems, the detector is composed of discrete sensing elements. The geometry and other characteristics of these detector elements (dels; Figure 4) play a large role in defining the imaging performance of the digital mammography system. In PSP systems, the sensor is continuous, but when it is scanned by a laser beam for readout, the size of the beam and the distance it sweeps between sample measurements define an effective del.

Tissue Coverage

Tissue coverage refers to the need to project as much of the breast tissue as possible onto an image; otherwise, a breast cancer may not be visualized. Tissue coverage depends on the chosen view (projection); the positioning of the breast; and the geometrical relationship of the x-ray source, collimation, compression device, patient, grid, and image receptor. The machine-dependent aspects of tissue coverage are illustrated in Figure 5. To maximize the inclusion of breast tissue in an image, the x-ray source must project a ray that is virtually tangential to the chest wall, intercepting the image receptor at the point closest to the chest wall. If the x-ray source is malpositioned (eg, after tube replacement), or if the collimation, compression plate, or grids are not properly aligned, tissue will be excluded from the image. Similarly, if the image receptor or its housing has an inactive region adjacent to the chest wall, tissue will be missed.

Typically, film mammography systems miss between

4 and 8 mm of tissue at the chest wall because of the front wall of the breast support and the edge of the cassette. All current digital units are also within this range, and this is desirable from a clinical perspective and should remain a minimum standard.

Tissue coverage can be clinically assessed by comparing the retromammary aspects of the breast between the craniocaudal and mediolateral oblique views. The distance between the nipple and the anterior edge of pectoralis muscle or the posterior edge of the image on the craniocaudal view should be not more than 1 cm less than the distance between the nipple and the pectoralis on the mediolateral oblique view. Also, the anterior edge of the mediolateral oblique image of the pectoralis muscle should be convex, and the muscle should be seen at least down to no less than 1 cm above the level of the nipple.

To assess the alignment of components that affect tissue coverage, a simple tool shown in Figure 6 can be used. This gauge is fixed to a plastic block or plate on which there is a “lip” representing the chest wall of the patient, such that when the plate is placed on the breast support surface, the lip engages the edge of the breast support. When it is imaged, it is possible to read directly the number of millimeters of tissue that is missed at the chest-wall side of the image.

For large breasts, the field of view of the mammographic detector may be insufficient to image the entire breast at once. In such situations, the breast must be imaged in sections, and the resulting subimages must be tiled together to form the complete mammogram. This procedure is identical to that used for film mammography. The larger the detector’s field of view is, the lower the probability that such multiple-section imaging will be required. Obtaining an image in a single view is desirable not only because the total acquisition time is minimized but also because of the possibility that slight changes in the breast configuration between views due to differences in compression direction could make the image sections difficult to match at the boundaries. Note also that the process of imaging the breast in sections results in an increase in radiation dose to regions of the breast that are exposed to x-rays in more than 1 subimage.

Spatial Resolution

Also referred to as “sharpness,” spatial resolution describes the ability of the imaging system to allow 2 adjacent structures to be visualized as separate. Alternatively, it can be used to describe the distinctness of an edge in an image.

The system spatial resolution can be assessed by imaging a bar pattern consisting of alternating radio-opaque “bars” and radiolucent “spaces” of equal width (Figure

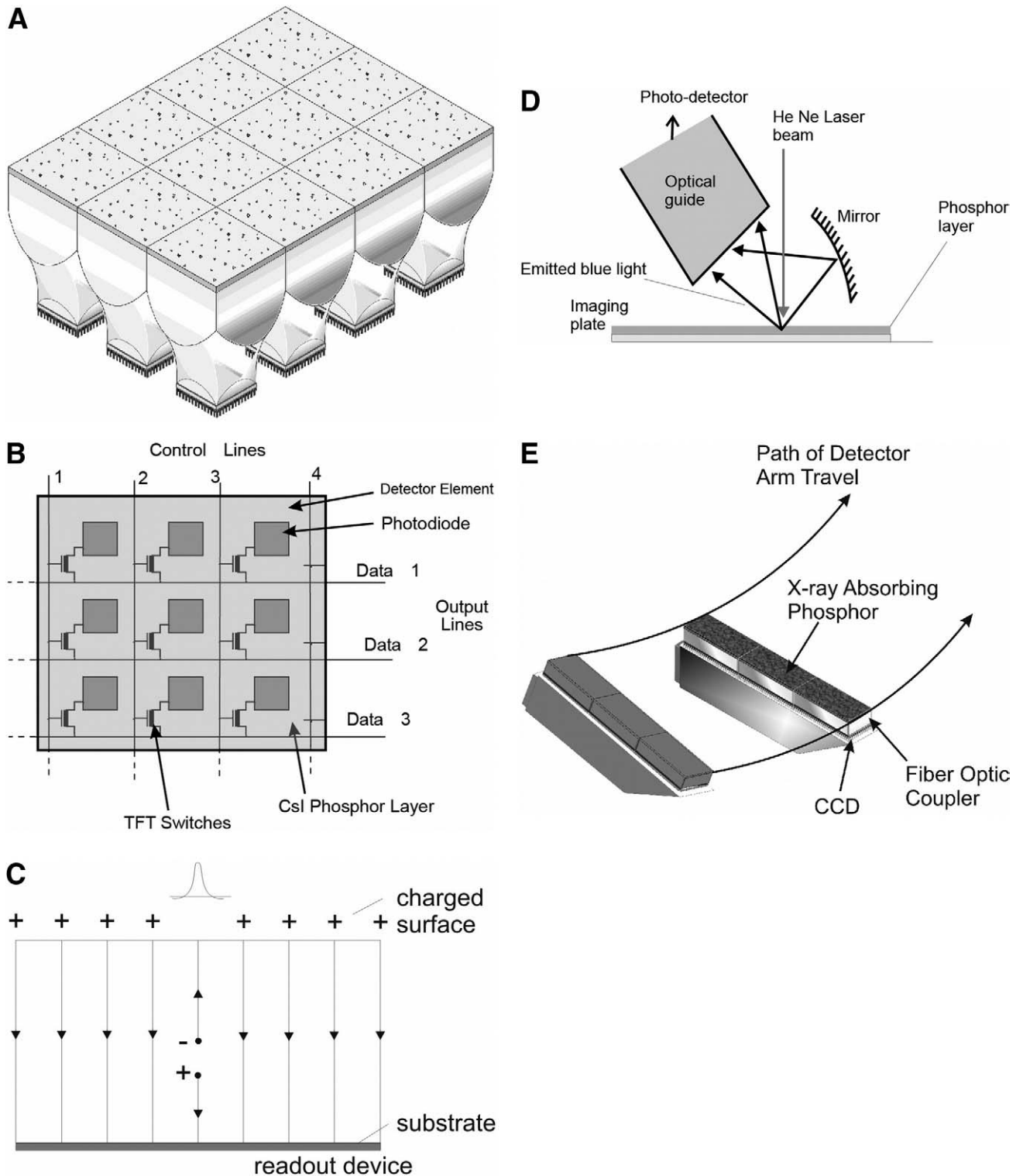


Fig 3. Current designs of digital mammography acquisition systems. (A) Large-area charge-coupled device (CCD; no longer commercially available): cesium iodide phosphor coupled to multiple CCD readouts through demagnifying fiber-optic tapers. (B) Photostimulated storage phosphor: photostimulable phosphor plate with dual-side laser scan readout. (C) Indirect flat-panel: cesium iodide phosphor on large-area amorphous silicon active-matrix photodiode array. (D) Scanned-slot CCD (no longer commercially available): cesium iodide coupled to multiple CCD modules through fiber optics. Acquisition through scanning x-ray beam and detector across the breast. (E) Direct flat-panel: amorphous selenium direct x-ray converter on large-area amorphous silicon active-matrix electrode readout. TFT = thin-film transistor.

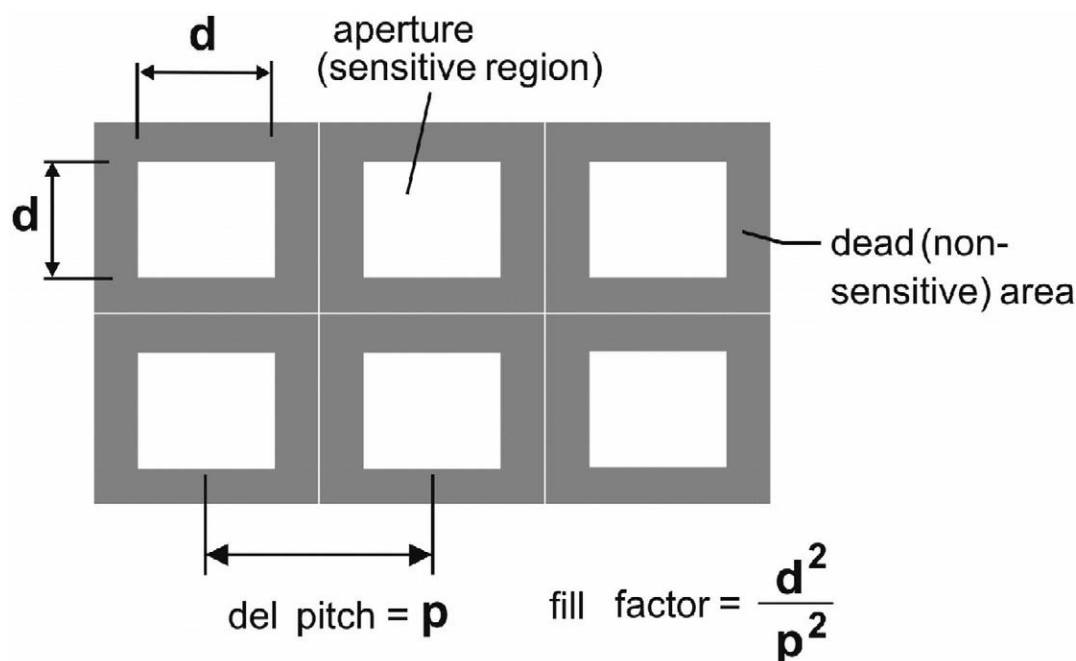


Fig 4. The detector element (del) determines, in part, the spatial resolution capability of the detector. The aperture, d , of the active area and the pitch, p , or spacing between elements are shown.

7). An adjacent bar and space are referred to as a line pair. In use, the pattern is imaged, and an observer determines the most closely spaced line pair for which 2 adjacent bars are seen as clearly separate. It is possible to perform the test so as to isolate and quantify individual blurring effects. For example, to measure the resolution of the image receptor, the bar pattern can be fixed firmly to the receptor so that there is negligible blurring due to motion or focal spot size. This is a subjective test, however, and is not very useful in the analysis of complex imaging systems.

A preferable measurement is the MTF [10]. The MTF describes how well an entire imaging system or a component, such as an image receptor or a subcomponent such as a phosphor, transfers the amplitude (analogous to contrast) of sinusoidal patterns from the incident x-ray pattern to the output. In a system containing several components affecting spatial resolution, the overall MTF can easily be calculated if the MTFs of the individual components are known. The system MTF is determined by multiplying at each spatial frequency the MTFs of the individual components. For example, as illustrated schematically in Figure 8, the MTF of a radiographic system is the product of that due to the focal spot, the detector, and any motion of the patient during the exposure. Determining which part of the system is responsible for limiting performance is thus possible.

Spatial resolution is limited by various sources of blurring. In digital mammography, these are primarily due to the size of the focal spot of the x-ray tube and the mag-

nification factor of a given structure of interest; unsharpness due to diffusion of light in the phosphor screen of the image receptor; the del effective aperture and pitch; and the relative motion of the x-ray source, the breast, or the image receptor during the exposure.

The size, shape, and intensity distribution of the x-ray tube focal spot in combination with focal spot-to-object and object-to-image receptor distances affect geometric blurring (Figure 9A). Each point in the focal spot casts a sharp shadow of structures within the breast. The size of the shadow increases with the degree of magnification between that structure and the plane of the image receptor. The entire focal spot can be thought of as a large number of adjacent point x-ray emitters. The overlap of the shadows from each causes blur. To minimize geometric blurring, the focal spot size and object-to-image receptor distance, d_2 , should be minimized, whereas the focal spot-to-object distance, d_1 , should be maximized.

Most mammographic procedures are performed with a moving Bucky-type grid. With the grid in place, there is a gap of 1 to 2 cm in distance between the exit surface of the breast and the image receptor. In modern mammographic units, the nominal focal spot size for most procedures is 0.3 mm. The convention of the National Electrical Manufacturers Association for defining nominal focal spot size allows the actual distribution of radiation to be considerably larger (1.5 to 2 times) than the nominal value. Also, the effective size of the spot varies over the image plane, being largest near the chest wall. Therefore, geometric resolution also varies over the image. For

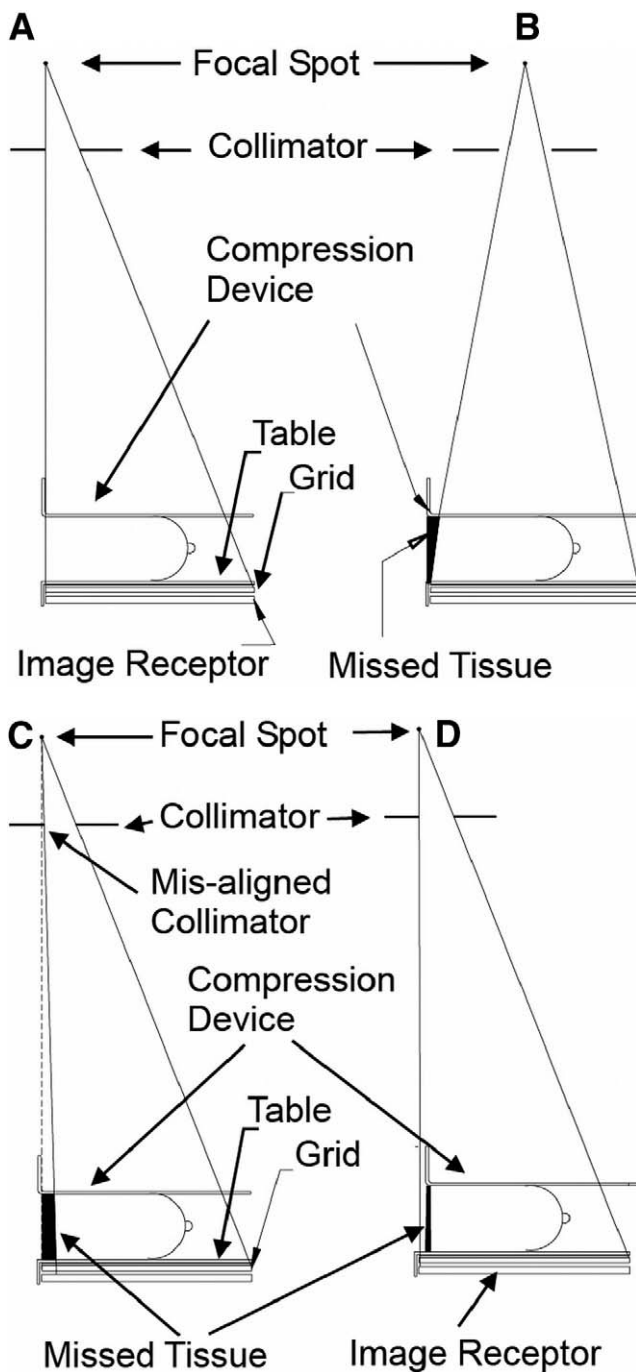


Fig 5. The effect of system geometry on tissue coverage near the chest wall. (A) Proper alignment causes the central ray from the x-ray source to be projected tangent to the chest wall. (B) Improper position of the x-ray source causes the image of some tissue proximal to the chest wall to be projected inside the patient's thorax. (C) Incorrect setting of the collimator or (D) incorrect positioning of the compression paddle or grid will also cause tissue to be missed.

geometric magnification, a second focal spot of nominal size (approximately 0.1 mm) should be used to avoid an unacceptable loss of resolution.

Factors affecting unsharpness for digital mammography referable to the detector itself are signal diffusion between dels, the active area of each del (aperture size), the pitch or center-to-center spacing between dels, and the pixel size used to display the image.

Most detectors are constructed as a set of discrete dels, as shown schematically in Figure 4. Each del has an active area with dimension d , and this may be surrounded by an area that is insensitive to the incident radiation. This causes the pitch, or spacing between dels, p , to be greater than d . For square dels, the relative area of sensitivity, d^2/p^2 is called the fill factor, and this in part determines the geometric radiation efficiency of the detector.

The del size also determines the basic spatial resolution associated with the del. Because information is "smeared" over d , the smaller d is, the less blurring results and therefore the higher the spatial resolution. As shown in Figure 10, the MTF associated with the del falls to zero at a spatial frequency of $1/d$ cycles/mm. A detector with 50- μm dels passes spatial frequencies up to 20 cycles/mm. Note that the MTF does rise again at frequencies beyond the first zero, but the information may not be reliably depicted beyond this point. For example, between the first and second zero points, there is a reversal of contrast, so that structures that should be dark appear light and vice versa.

The pitch is also important in affecting image quality. The spacing between samples determines whether information is lost between measurements. If this occurs, a phenomenon called aliasing can result. To avoid aliasing, the highest spatial frequency of information in the image, f_{max} , must be less than $1/(2p)$, which is referred to as the sampling frequency. Otherwise, aliasing causes information at spatial frequencies greater than $1/(2p)$ to be represented at lower spatial frequency, as illustrated in Figure 11. In Figure 11A are 2 sinusoidal patterns, 1 of low frequency and 1 of higher frequency, and the image in which both patterns are combined where there is no limitation due to sampling. Both patterns are seen clearly in the combined image. When the sampling pitch is too great, as in Figure 11B, we see that not only is the higher spatial frequency information poorly imaged, but the resulting erroneous (aliased) information that it produces at the lower spatial frequency also interferes with the proper representation of the lower frequency object. Therefore, for example, although 50- μm dels will pass information up to 20 cycles/mm, they provide unaliased imaging only up to 10 cycles/mm. Any content in the image beyond 10 cycles/mm will cause aliasing to affect lower frequencies.

Note that resolution specifications based on d and p

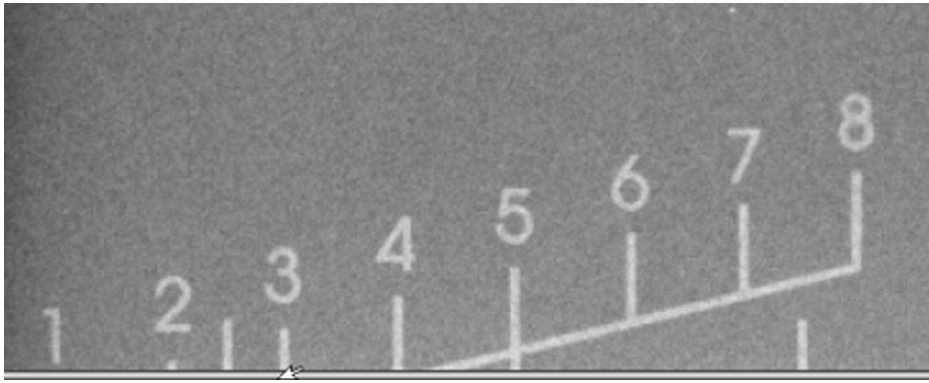


Fig 6. Device to measure the amount of tissue missed at the chest wall. On this system, 4.2 mm are cut off from the image.

apply only to the directions parallel to the rows and columns of the image. For other directions, resolution will be lower. For example, at 45°, the aperture and pitch will be about 40% greater than along the principal axes,

and the resolution and aliasing will be affected accordingly.

The MTF for a digital detector is determined partially by the effective del aperture and partly by physical signal spread between dels. The design philosophy for digital mammography balances many factors, including trade-offs between spatial resolution, SNR, and radiation dose requirements, as well as manufacturing and economic considerations. The hypothesis of the design is that the improved dynamic range and SNR provided by digital mammography will outweigh a loss of limiting spatial resolution, and therefore, the del pitch has been chosen by different manufacturers to provide sampling frequencies between 5 and 10 cycles/mm. To isolate the amount

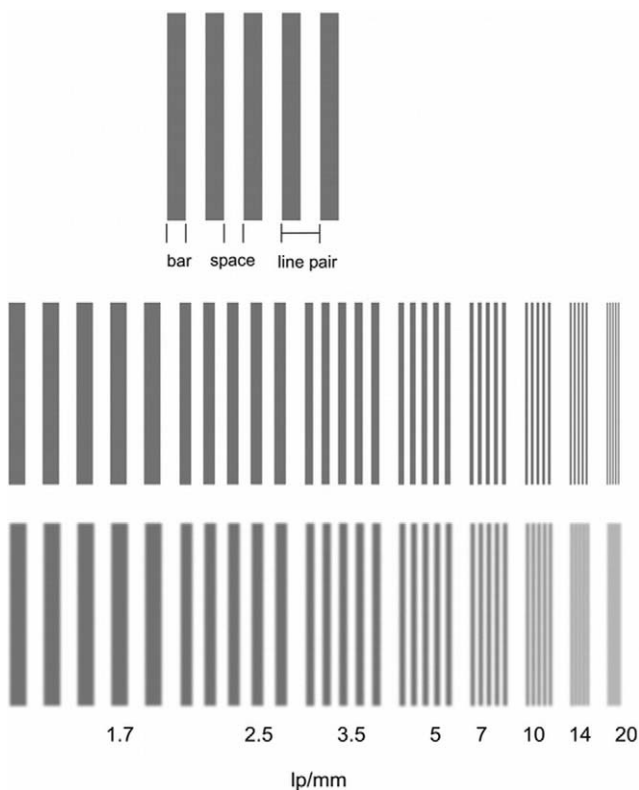


Fig 7. Measurement of spatial resolution with a bar pattern test. From the top of the image, the first row illustrates the concept of line pairs (lp) per millimeter, the second row demonstrates a pattern containing sections spanning a range of line pairs per millimeter, and the third row illustrates the effects of an unsharp imaging system on the resolution of the bars.

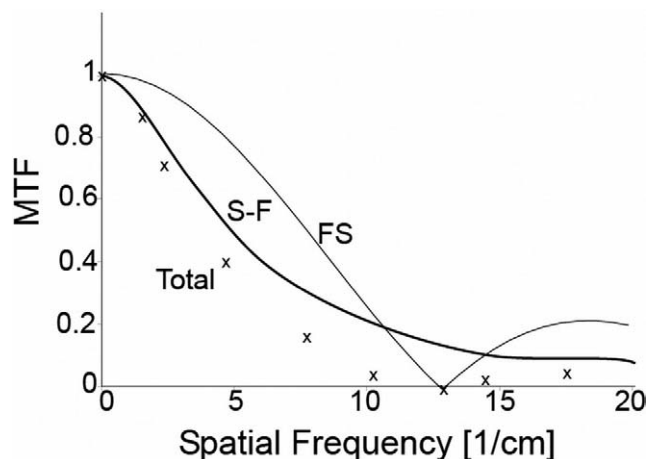


Fig 8. Modulation transfer function (MTF). This figure describes how well an imaging system conveys the modulation or contrast from the input to the output. The curve labeled “S-F” shows the MTF of a mammographic screen-film system, and the curve labeled “FS” shows the MTF due to the smaller focal spot and geometric magnification. The overall MTF, including both effects is shown, by the x values.

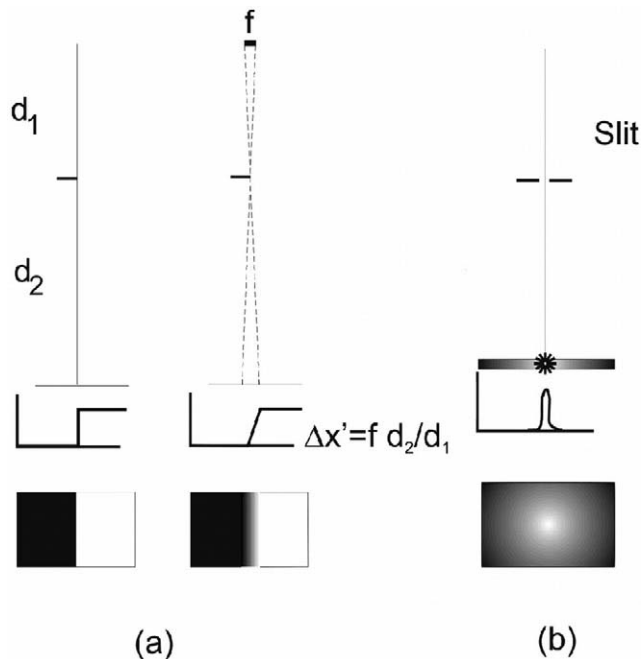


Fig 9. Some of the sources of image blurring in mammography. (A) Geometric unsharpness due to the focal spot and magnification. (B) Unsharpness due to the lateral spread of signal (eg, light produced in a phosphor) in the image receptor.

of intrinsic blurring caused by the detector from the effects of sampling, it is customary to measure the MTF before sampling or pixilation occurs and to specify the “presampling MTF” of the detector. This measurement can be done by imaging a sharp edge or a narrow slit that is tilted by a small angle with respect to the principal axes of the detector [11]. By combining measurements of this edge spread function or line spread function from several rows of the image, it is possible to simulate sampling at an interval much finer than the del pitch. The presampling MTFs for several digital mammography systems are shown in Figure 12.

Another factor that increases image blur is long exposure time, which may result in patient motion. In digital mammography, most motion blurring is caused by movement of the breast during exposure. It can be minimized by using a short exposure time and by compressing the breast. Settings of kilovolt potential may be increased for thick, dense breasts to allow the reduction of exposure time. Magnification techniques generally require longer exposure times because small focal spots with lower tube current (milliamperes) capacity are used. The amount of blurring depends on the speed of the motion in the patient and the duration of the exposure (Figure 13). For consideration of blur, the exposure time in the case of the large-area digital systems is the complete exposure time, whereas for a scanned-slot charge-coupled

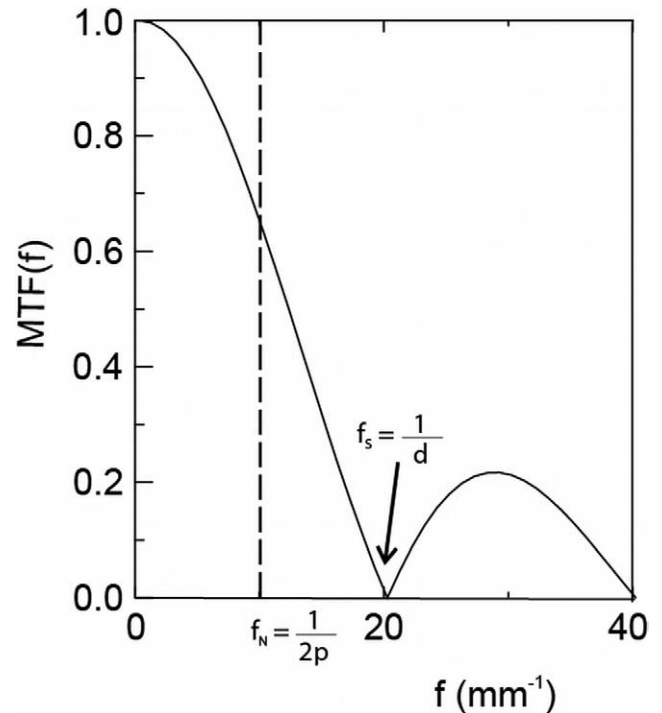


Fig 10. MTF associated with the del size, d . In this example, $d = 50 \mu\text{m}$, $f =$ spatial frequency; $f_N =$ sampling frequency; $f_s =$ cut off frequency due to del size, d ; $p =$ pitch. MTF associated with the size, d .

device (SSCCD) system, only part of the breast is exposed at any time. Even though the overall exposure time is generally longer for a scanning system, the time that x-rays expose a particular part of the breast (ie, the time that affects blurring) is only a small fraction of the total exposure time. For scanning systems, motion can, however, cause misregistration artifacts between the anatomy that is imaged before a motion occurs and that imaged after.

For a given image receptor sensitivity (a specified amount of radiation required at the image plane), there is a trade-off between motion blur and geometric unsharpness. If one attempts to reduce motion blur, a greater x-ray output must be available. This is normally accomplished by increasing the tube current or reducing the distance from x-ray tube to image receptor. The former requires increasing the focal spot size. In either case, geometric unsharpness will become greater. Reducing distances also makes patient positioning for the examination more difficult. With digital mammography, an alternative approach may be to increase tube kilovoltage, because the loss in contrast may be compensated for by adjustment of the image display.

In addition, it is useful to consider the mechanisms operating on spatial resolution in the different detector systems. For SSCCDs or indirect flat-panel (IFP) sys-

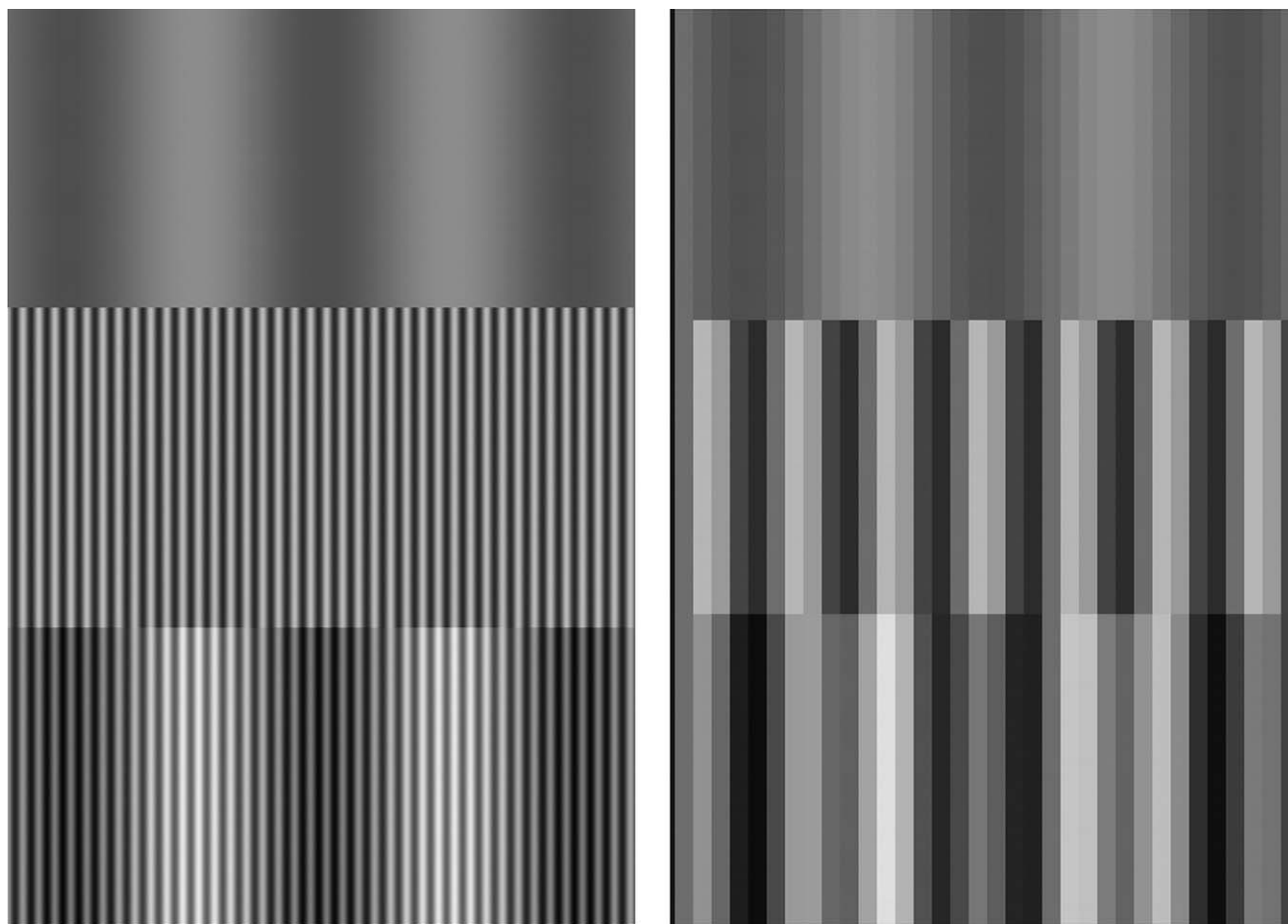


Fig 11. Aliasing. (A) Pattern containing sine waves at 2 spatial frequencies and their summation. (B) The effect of undersampling, which causes the higher spatial frequency pattern to be unresolved and also causes the higher frequency pattern to disturb the lower frequency pattern, which would otherwise be imaged correctly.

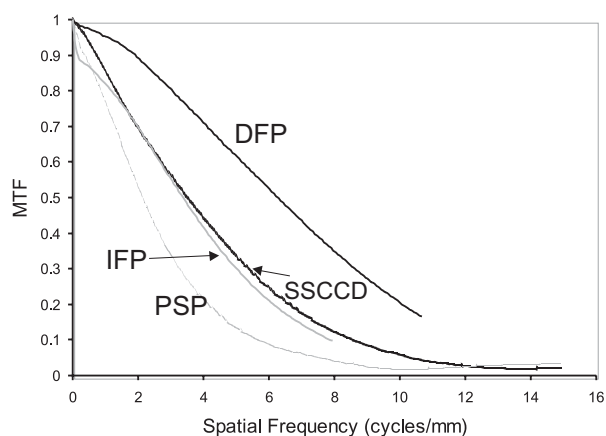


Fig 12. Presampled modulation transfer functions (MTFs) for various current digital mammography detectors.

tems, the first source of blur that occurs is spreading of emitted light within the cesium iodide crystals. This is determined both by the thickness of the phosphor (sharpness can be exchanged for quantum efficiency) and by the engineering of the phosphor (crystal structure, reflective and absorptive materials). The latter are closely guarded secrets of the manufacturers. In SSCCD systems, the quality of the fiberoptic coupling of light between the phosphor and the charge-coupled device (CCD), specifically, any deviation in the one-to-one correspondence of fibers between the entrance and exit surfaces of the coupler due to twisting, warping, and so on, will also affect resolution. In direct flat-panel detectors, the field across the direct conversion material must be adequate to ensure that there is negligible lateral spreading of charge created in the material before it is collected at the electrodes.

The spatial resolution is affected by the aperture and pitch of the dels in the readout device, namely, the CCD cells or the photodiode or electrode elements in flat panel devices using thin-film transistor arrays.

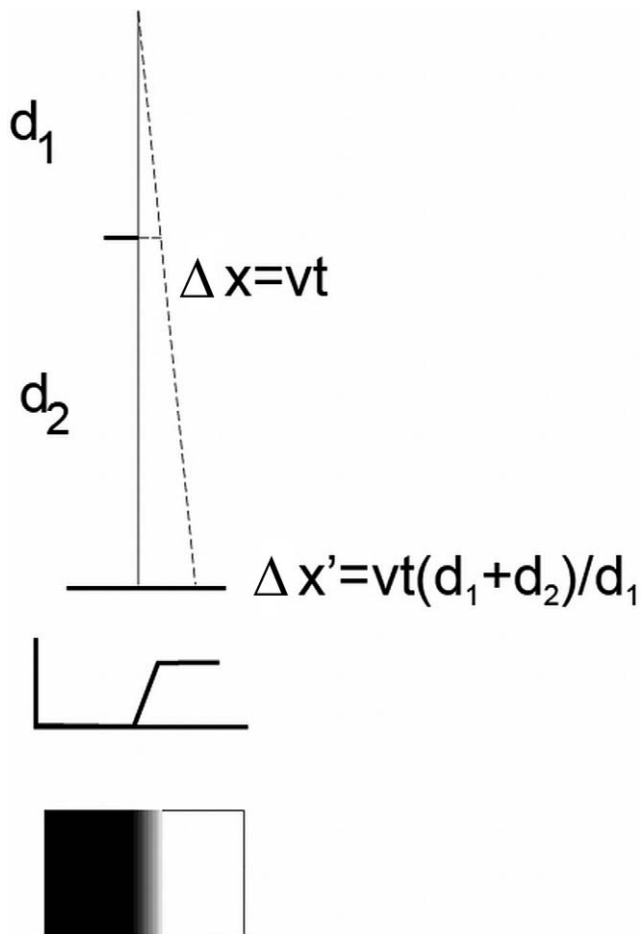


Fig 13. Motion unsharpness is due to relative motion between the x-ray source, structures within the breast, and the image receptor during image acquisition. It is determined by the velocity of motion and the exposure time per detector element.

In an SSCCD system, the detector moves across the breast while the charge in the CCD elements is shifted down the columns of the CCD at the same speed as but in the opposite direction of the detector motion. The matching of the mechanical and electrical transfer speeds is critical, because a mismatch will cause blur. Any inefficiency of charge transfer in the CCD will cause additional blurring. There is also a minor effect on resolution because the detector moves continuously, whereas the charges are shifted in discrete jumps through the phases of each CCD element and from row to row down the columns.

Although the readout structures of IFP and direct flat-panel devices are very similar, there is an important difference between the collection of light and charge, which can provide both advantages and disadvantages. For example, in IFP detectors, only the light produced in the phosphor above the active area of each del will be mea-

sured. In direct flat-panel detectors, charge travels along electric field lines, so that the charge produced in a region above an inactive part of the del can be redirected by the shape of the field to fall on the active electrode area. This makes the effective fill factor for the del higher than it would otherwise have been. On the other hand, a detector composed of adjacent dels will always suffer from undersampling, so that aliasing will occur unless some multiple sampling strategy is used. This is generally too time consuming and complex to be practical. The spreading of light in an IFP detector may provide adequate blurring of the high-spatial-frequency information to reduce the amount of aliasing compared with the sharper direct conversion detector of the same del dimensions.

The mechanisms determining the resolution characteristics of PSP detectors are quite different from the others. Although this is a phosphor system, the spread of light produced by the phosphor is not of concern, because the emitted light is not used to provide spatial localization. Instead, the spatial information (ie, the effective del) is determined by the size of the scanned laser beam on the imaging plate used in the readout and the distance that the beam is moved (pitch) between successive lines of the laser-stimulated light. Light produced by the phosphor when the traps are emptied by the energy from the laser light must be collected as efficiently as possible. The effective size of the laser beam is determined by the actual beam size as well as the amount of scattering of the laser light that takes place within the phosphor. This determines the point spread function from which the MTF due to the laser can be calculated. The uniformity of motion of the scanning beam and the indexing of the phosphor plate also have an effect on the resolution and uniformity of the image.

The effect of spatial resolution is most easily observed when considering the imaging of fine detail in the breast, such as spiculations radiating from a mass or calcifications. In addition to allowing the detection of calcifications, high spatial resolution is necessary to provide information on their shape and margin to assess whether their cause is more likely to result from a benign or malignant process. Calcifications are the most common presentation of the ductal carcinoma in situ, an early form of breast cancer confined to the duct itself. In [Figure 14](#), a region of a digital mammogram containing calcifications is shown. In [Figure 14A](#), the calcifications are depicted with a very high spatial resolution. In [Figure 14B](#), they have been blurred in the manner that would occur if a system with a 50- μm del were used to acquire the image, while [Figures 14C](#) and [14D](#) represent 100- μm and 200- μm dels, respectively.

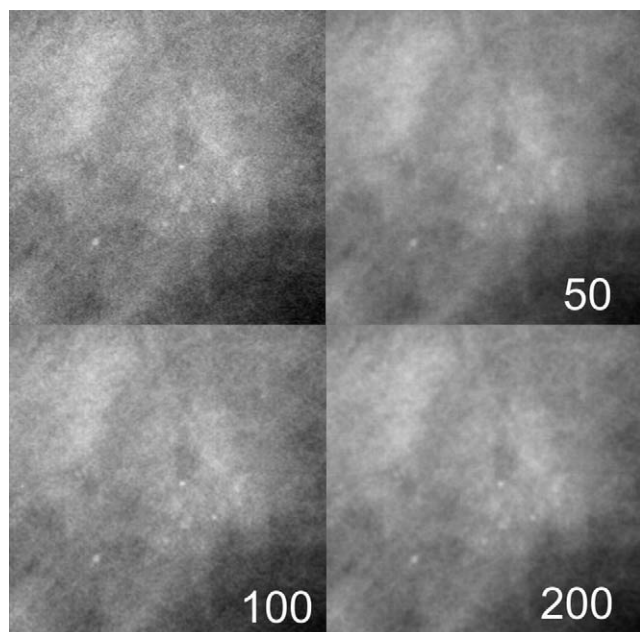


Fig 14. Effect of del size on the spatial resolution of microcalcifications. Top left: Calcifications depicted with high spatial resolution. Top right: Blurring of image that would occur with a system that used 50 μm dels. Bottom left: image with 100 μm dels. Bottom right: Image with 200 μm dels.

Radiographic Contrast

Radiographic contrast is the magnitude of the signal difference between the structure of interest and its surroundings in the displayed image. Radiographic contrast is influenced by 2 factors: subject contrast and display contrast. Contrast is typically considered for larger areas ($\geq 1 \text{ cm}^2$) in an image. Subject contrast is measured in terms of the relative difference in x-ray exposure to the image receptor, transmitted through one part of the breast and through an adjacent part, whereas overall radiographic contrast, which depends on both the subject contrast and the display contrast, is expressed in terms of the optical density difference between 2 areas on the processed laser film or as the relative brightness difference between the corresponding areas in an image displayed on a monitor.

Subject contrast is especially important in mammography because of the subtle differences in the soft-tissue density of normal and pathologic structures of the breast and because of the importance of detecting minute details such as calcifications and the marginal structural characteristics of soft-tissue masses. Subject contrast is caused by differences in the x-ray attenuation properties of the lesion and those of the surrounding tissue. There is less inherent subject contrast in breasts than elsewhere in the body, because there are no bony structures or gas. Cancers and fibroglandular tissue can show similar x-ray

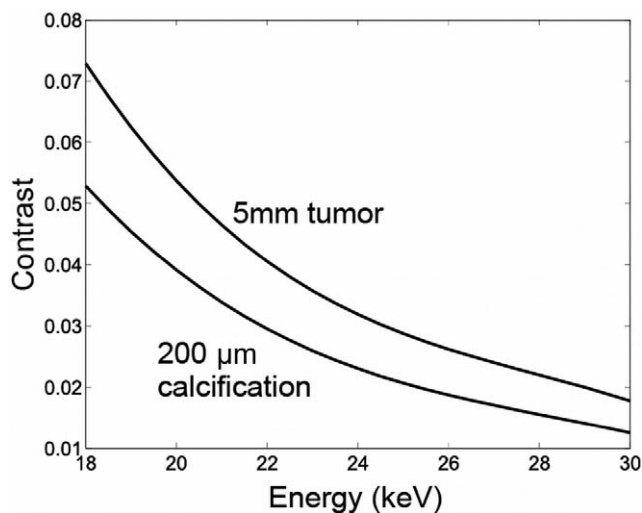


Fig 15. Calculated subject contrast for a small tumor and for calcifications compared with the x-ray energy used for imaging.

attenuation (defined here as mass per unit volume) because of the similarity in the atomic number of lesions relative to normal tissue. These differences and therefore the contrast also depend on the distribution of x-ray energies (spectrum) used for producing the mammogram. The x-ray spectrum is determined by the tube target material, kilovolt potential setting, and filtration (either inherent in the tube or added in its exit port). Figure 15 illustrates how the subject contrast of a tumor and calcification decrease as the energies of the x-rays increase.

Maximizing subject contrast is particularly important. Most commonly, molybdenum target x-ray units are used. These provide high radiation output at the characteristic emission energies for molybdenum of 17.9 and 19.5 keV. When a molybdenum filter (typically 0.025 to 0.03 mm) is used, the spectrum is strongly suppressed at lower photon energies and at energies greater than 20 keV because of the strong increase in x-ray absorption by molybdenum that occurs at its k-shell absorption edge. Therefore, the spectrum is rich in photons at and near the characteristic energies. These energies yield high subject contrast while avoiding the excessive radiation dose for breasts of average thickness, which would occur at lower energies.

For thicker, denser breasts, few low-energy photons are able to pass through the breast and, because of the greater filtering action of a thick dense breast, absorption differences among structures become smaller in the resulting harder (or higher average energy) x-ray beam. Therefore, subject contrast is not as high as with average-size or fatty breasts. In addition, as a dose-saving measure, higher energy incident x-ray beams are typically used to image these breasts. Although the effective energy

can be adjusted by varying kilovoltage, the effect on the spectrum is somewhat limited because of the dominance of the fixed-energy characteristic x-rays from the target. This motivates the use of targets and filters of different materials to tune the spectral shape. Rhodium has a K-absorption edge at 23 keV, and a rhodium filter will pass energies between 20 and 23 keV. Used with a molybdenum target in combination with an increase in kilovoltage, this will give a more penetrating spectrum than that obtained with the molybdenum-molybdenum combination. This can be helpful in imaging thick breasts (>5 or 6 cm) of fatty or average composition.

If an even more penetrating beam than available with molybdenum-rhodium is desired, it is possible to use a rhodium target in combination with a rhodium filter. Rhodium has characteristic emissions at 20 and 23 keV. The rhodium-rhodium combination is most effective with very dense, difficult-to-penetrate breasts, providing some dose reduction while preserving as much subject contrast as possible in these difficult-to-image breasts. It is also possible to provide a suitable spectrum for imaging dense breasts with a tungsten target tube and various metallic filters such as rhodium. Although this does not provide the quasi-monoenergetic x-rays available with the molybdenum and rhodium targets, careful choice of kilovoltage and filter material and thickness can yield an excellent result in terms of contrast and dose.

For digital systems, the ability to adjust display contrast may make it advantageous to use slightly higher energy x-ray beams than are used with film mammography (for which 22 to 32 kVp is typically used, depending on the thickness and density of the breast). Provided that an adequate SNR is maintained, this may provide a dose reduction compared with screen-film mammography, especially for large or dense breasts. Digital Mammographic Imaging Screening Trial data suggest that this can be accomplished with improved diagnostic accuracy [12].

Another source of contrast degradation for digital mammography is the presence of scatter radiation. In soft tissue, even at the low energies used in mammography, scattering is an important mechanism by which x-rays interact with breast tissue. Scattered x-rays that escape the breast and are recorded by the image receptor reduce image contrast and the apparent sharpness. The amount of scattered radiation recorded compared with the useful, directly transmitted x-ray intensity, is characterized by the scatter-to-primary ratio. It is not unusual for the scatter-to-primary ratio to be greater than 1.0 [13,14]. For film systems, scattered x-rays recorded by the image receptor reduce the value of subject contrast, use up some of the available recording range or latitude of the film in recording essentially useless information, and add noise

to the image, thereby reducing its SNR, which is a measure of the information content of the mammogram.

In digital mammography, the same factors apply, but the effect of scattered radiation on the final radiographic contrast is somewhat different. Because x-rays may scatter multiple times within the breast, their spatial distribution is diffuse (ie, mainly affecting the low-spatial-frequency part of the MTF). For this reason, in digital systems, much of the contrast can be recovered by viewer adjustment of the computer image display. Similarly, the system can be designed such that the dynamic range of the image receptor is very large, so that recording of scattered radiation will not be a limiting factor. Under these conditions, only the third effect, the addition of random quantum noise, should be of any importance.

The use of specifically designed grids for mammography reduces the amount of scattered radiation detected and improves subject contrast. This is particularly important when imaging thick, dense breasts [15,16]. Grids, consisting of lead strips separated by spacers of radiolucent material, are a standard feature of modern mammographic x-ray units. Most of these grids are 1-D and move during the x-ray exposure to allow for blurring of the image of the grid septa, rendering them invisible. Alternatively, one manufacturer provides a 2-D focused rhombic cellular structure grid in which the interspace material is air. These grids offer the potential of improved image contrast and transmission efficiency compared with conventional grids. For all digital systems except SSCCD systems, grids are typically used, because of the reduction in noise due to the scattered radiation and the consequent increase in the SNR. With a digital system, any exposure increase necessitated by the use of the grid is due only to its incomplete transmission of the primary radiation. An SSCCD system uses a narrow scanned beam of x-rays, which reduces the scatter-to-primary ratio. In addition, the long, narrow detector with collimation at its entrance surface rejects much of whatever scattered radiation is incident on the detector. Currently, a grid is not used with this system, and exposures can be lower.

Subject contrast should also be optimized by good breast compression. Compression is an important factor in reducing scattered radiation. In a study using phantoms, Barnes and Brezovich [13] showed that reducing the thickness from 6 to 3 cm by compression reduced the scatter-to-primary ratio from 0.8 to 0.4. The use of a mammographic grid further reduced the scatter-to-primary ratio to 0.14. In addition, compression can provide several other technical improvements in image quality, which can be achieved without compromising other image quality factors. These improvements include the immobilization of the breast, which reduces blurring caused by motion; the location of structures in the breast closer

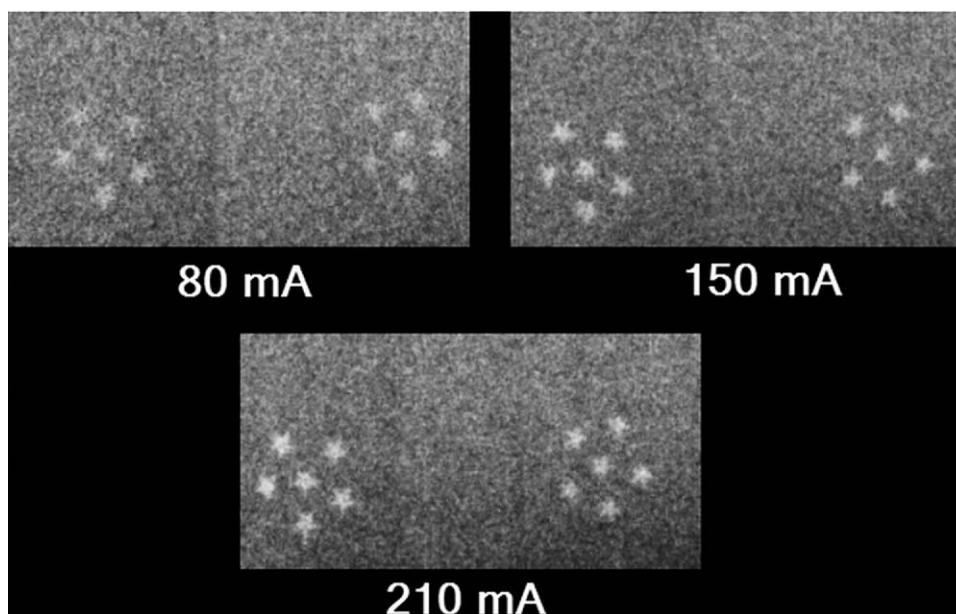


Fig 16. The influence of the quantity of x-rays used to make a mammogram on its quality and the reliability of characterizing structures containing fine detail. Increasing milliamperage decreases the relative magnitude of noise and improves diagnostic detail.

to the image receptor, which reduces geometric blurring; the production of a more uniformly thick breast, which in turn results in more even penetration by x-radiation and less difference in radiographic density in the area between the chest wall and the nipple; the reduction of radiation dose; and, finally, the spreading of breast tissue, enabling suspicious lesions to be more easily identified.

Finally, for digital mammography, the signal stored in digital form is directly (or logarithmically) proportional to the amount of radiation transmitted through the breast. With a properly designed image acquisition system, the dynamic range should be adequate to measure the entire range of intensities from that of the unattenuated beam outside the breast to that through the densest, thickest part of the breast. For this reason, the stored image reflects the inherent subject contrast very faithfully.

Noise

In digital mammography, it is not very meaningful to discuss contrast without also considering noise. Radiographic noise or mottle is the unwanted variation in random optical density in a radiograph that has been given a uniform x-ray exposure [17-19]. Quantum mottle is caused by the random spatial variation of the x-ray quanta absorbed in the image receptor, and its effect is reduced as more x-rays are used to form the image. The effect of using fewer quanta on noise and on perception of subtle contrasts can also be seen in Figure 16, in which digital images have been produced of a phantom containing star-shaped objects mimicking calcifications.

Noise can be quantified in terms of the standard deviation of the number of x-ray quanta recorded in a given area of the image receptor or the standard deviation in image signal (optical density or digital image value) over a given area (region of interest) of the image. This says nothing, however, about the spatial characteristics of the noise. This is better described by the noise power spectrum of the image [20,21].

More important than the absolute noise level is the consideration of the relative magnitudes of the noise and the image signal. This is described by the SNR or more commonly, the signal-to-noise transfer efficiency or detective quantum efficiency of the image [1,21-23]. Detective quantum efficiency describes the transfer of the SNR from the x-ray pattern incident on the imaging system to its output. It is generally plotted against spatial frequency, as shown in Figure 17. Figure 18 illustrates the effect of noise in imaging a dense breast. Because an insufficient amount of radiation is transmitted through the breast, the mammogram is quite noisy, making the reliable detection of small structures, such as calcifications, difficult. It is extremely important that an adequate x-ray exposure is used to ensure that detection and characterization of lesions will not be impaired by the presence of noise. An effective automatic exposure control system is valuable in helping achieve this goal.

A structure in the breast must be visualized with respect to its surroundings, so it is useful to calculate the ratio of the signal difference (the difference in image value between 2 points of interest) to the noise in that difference. This is described by the signal difference-to-

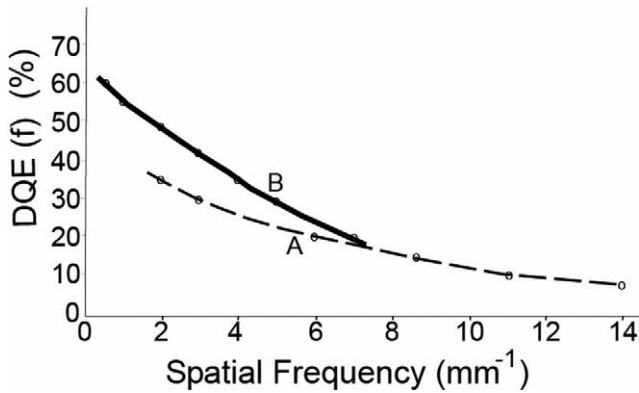


Fig 17. Detective quantum efficiency (DQE) versus spatial frequency for A, a modern mammographic screen-film image receptor, and B, a digital mammography detector (direct flat-panel [DFP]).

noise ratio (SDNR) of the image. To reliably detect a structure in the breast in the presence of noise, the SDNR must exceed some threshold value, typically 5. Calculated values of the SDNR are presented in Figures 19A and 19B for the case of detection of a small mass and calcifications, respectively, in breasts of different thicknesses. Note that for typical radiation exposure levels used in mammography, the SDNR is more than adequate for the mass but may be marginal for the calcifications. A simple method of measuring SDNR and an example of measurements are illustrated in Figure 20.

Quantum noise should be the principal contributor to the signal fluctuation seen in a uniformly exposed radiograph. Factors affecting the perception of quantum mot-

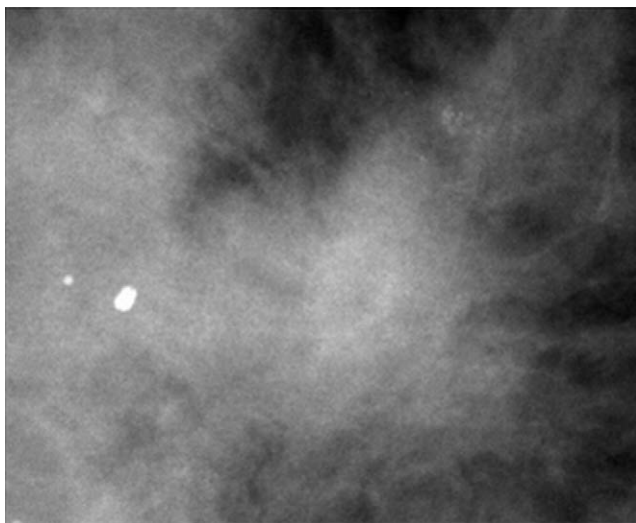


Fig 18. The impact of excessive quantum noise due to underexposure on the quality of a digital mammogram. Noise interferes with detection and characterization of calcifications.

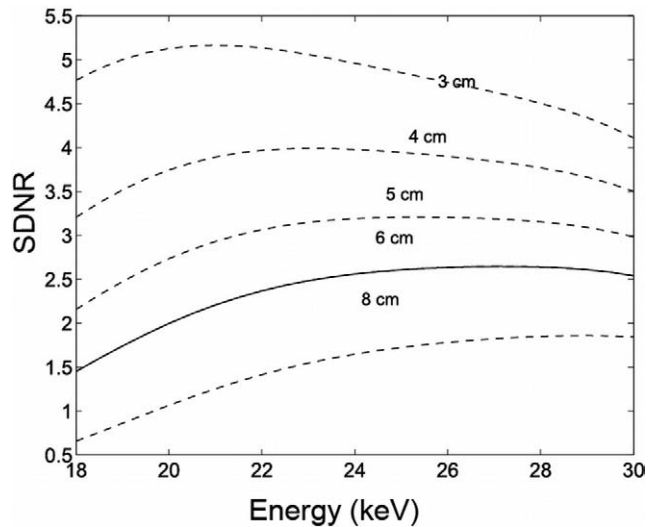
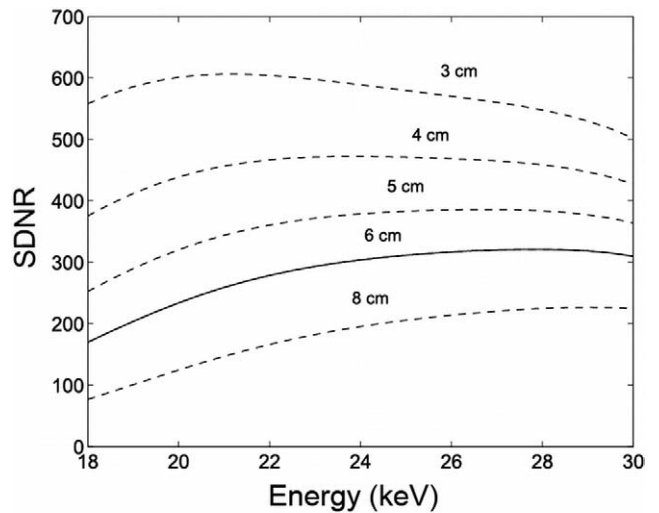


Fig 19. Calculated signal difference-to-noise ratios (SDNRs) versus effective x-ray energy for different thicknesses of 50% fat and 50% fibroglandular tissue for a 5 mm diameter tumor (A) and 200- μ m calcifications (B) in compressed breasts ranging in thickness from 3 to 8 cm.

tle in mammography include x-ray interaction efficiency, efficiency of converting x-rays to light or electrons and collecting the signal, light diffusion in phosphors, and radiation quality. When sensitivity is increased because of increased x-ray absorption (higher quantum efficiency) for a given detector output, quantum mottle is not increased. When speed is increased because of other amplification mechanisms, fewer x-rays are used to form the image, and therefore quantum mottle is increased. Spreading of signal in the detector blurs the recording of quantum noise, so that it becomes less apparent but also causes a decrease in spatial resolution. Higher energy x-rays are absorbed with lower quantum efficiency, resulting in a noisier image for a given number of x-rays

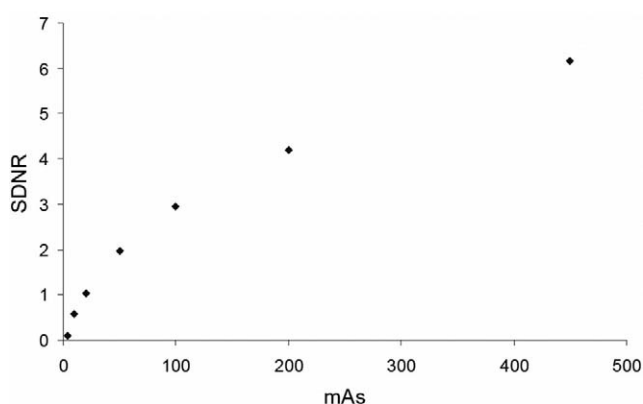
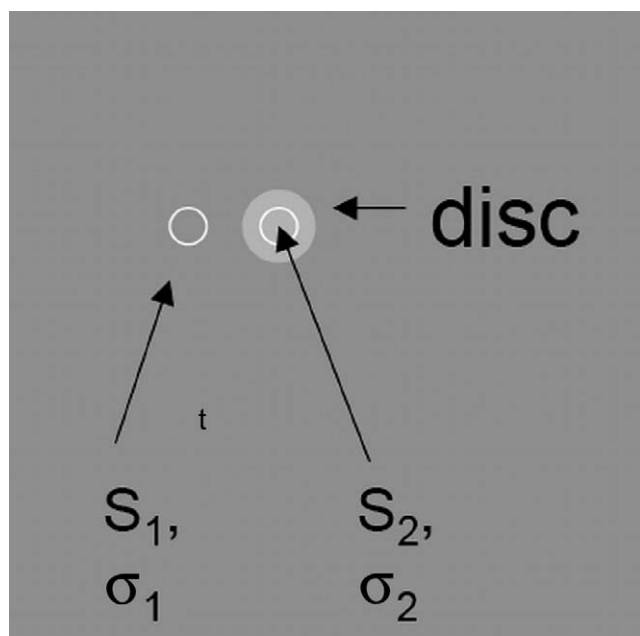


Fig 20. A simple test object for the measurement of the signal difference-to-noise ratio (SDNR).

transmitted through the breast. More important, they produce more secondary quanta per x-ray, so that a given signal (pixel value) can be achieved with fewer x-ray photons (ie, higher noise).

For mammographic imaging systems, quantum noise is a fundamental factor that can never be eliminated, only minimized. This is accomplished by attempting to maximize quantum efficiency and by using an adequate radiation dose. In digital mammography, the detector and electronics should be designed to have adequate dynamic range and number of bits of digitization to precisely record the entire range of x-ray intensities transmitted by the breast. If this is the case, the electronic image can be amplified as much as desired so that there is really no constraint on image brightness. If an inadequate number of quanta are used, however, the SDNR will be inadequate, and it is really the desired SDNR that should

determine the radiation dose used for a given examination.

In digital mammography there may be spatial variations in sensitivity of the receptor, which would cause an image to have structure that is unrelated to the tissues in the breast. As long as the system design ensures that these variations are temporally stable, this “fixed pattern noise” can be eliminated by imaging a uniform field of x-rays and using the recorded image as a correction mask to make the image uniform (Figure 21). This procedure is often referred to as flat-field correction [24].

The Elimination of Artifacts and Other Image Quality Problems

Acquisition processing (also known as image preprocessing) represents the manipulation of the direct output of a digital detector to correct for dead dels, nonfunctional columns or rows, stationary structured noise patterns, local gain variations, background (no signal) offsets, and global nonuniform response. Detector imperfections produce added noise in an output image that can overwhelm the signal variations inherent in the recorded x-ray image. Variations in the incident x-ray beam caused by the x-ray equipment itself (eg, the heel effect, added beam filtration, and grid transmission) can also detrimentally affect the output image quality. In some cases, corrections are possible for a fixed x-ray tube or detector geometry.

Correction algorithms are specific to the type of digital detector. For all digital systems with discrete dels (the exception being cassette-based PSP detectors), initial corrections require the identification of the locations of dead or transient element responses, as well as row and column defects. A map is determined and the averaged response of adjacent dels is substituted into the bad del. More than 1 adjacent dead element, dead column, or dead row makes this correction potentially unsatisfactory, particularly if in the central area of the detector matrix, where diagnostic information is most crucial. The number of nonfunctional dels (both adjacent and nonadjacent) determines the acceptability of the detector. Over time, some dels might lose functionality, which will require a reanalysis of the “bad-element map.” A trigger for such an evaluation occurs when dropouts become visible in the processed digital images or flat-field images.

Subsequent acquisition processing correction schemes are classified into 1-D and 2-D methods and typically require a linear (or modifiable linear) response over the useful dynamic range of the detector (eg, twice the incident radiation exposure results in twice the corresponding digital output value). Uncorrected digital detector response is determined by acquiring images with unattenuated or uniformly attenuated x-ray beam fluence of high incident exposure to reduce the quantum noise vari-

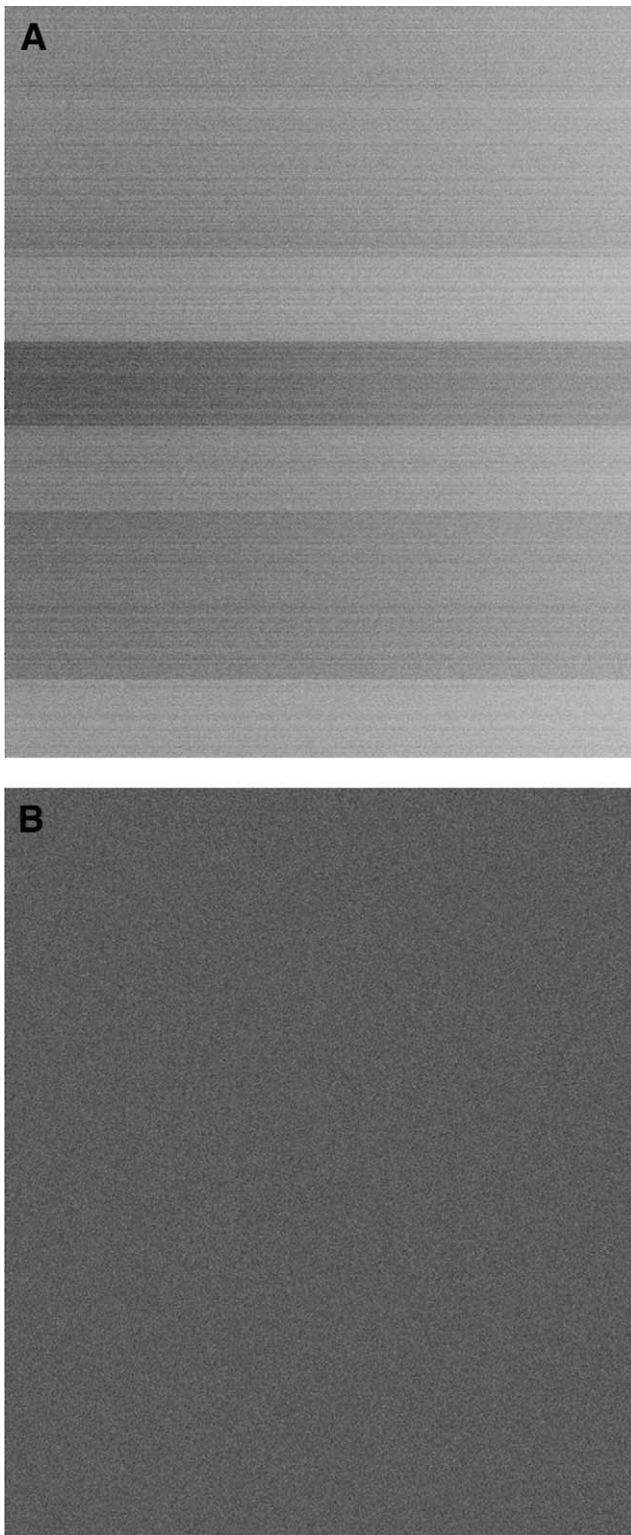


Fig 21. The effect of flat-fielding correction. (A) The raw image. (B) The same image after flat-field correction.

ability. For mammography, the x-ray beam is typically nonuniform because of heel-effect intensity variations, falling off significantly toward the anode (nipple side) of the field.

Cassette-based PSP and SSCCD arrays use a 1-D based correction method. For PSP systems, gain variations are chiefly due to the pickup light guide, and the correction is applied in the scan direction only.

For PSP, future 2-D correction methods could be used (above and beyond the 1-D corrections for the PSP reader response variations) by evaluating the response of each uniformly exposed imaging plate (after 1-D corrections are applied) and using methods described below for corrections of nonuniform response in 2 dimensions. This would require each PSP imaging plate in the inventory to have a 2-D correction map. In addition, because of the positional variability of the imaging plate within the mechanical translation device, the corrections would likely be applicable to the low spatial frequency spectrum and correct global variations but not local variations.

Two-D correction techniques, often called flat-fielding, generally involve dividing each image by a mask image. If the mask image is not acquired with sufficient radiation, it will be noisy, and this noise will propagate into the corrected image. In addition, there can be noise associated with the electronic circuitry that amplifies and digitizes the detector signal. For a digital system to perform well, it must be designed to minimize these non-quantum noise sources such that the SNR is determined by the level of radiation used. As an example, the measured detective quantum efficiency for a direct amorphous selenium thin-film transistor array, based on the results of Yorker et al [25], is shown as curve B in Figure 17.

The frequency of 1-D or 2-D calibration is dependent on the type of digital detector and recommendations for quality control (QC) by the manufacturer. For instance, daily calibration (or before patient use) is recommended for a digital mammography biopsy system using a fiber-optic taper-CCD sensor, with yearly (or as needed) for 1-D corrections for PSP systems and all other digital detector systems falling within that range. The basis for the calibration frequency is dependent on the amount of potential drift of the detector response at any time relative to the correction matrix acquisition time. Certainly, any drift or variation from the calibrated values will result in an incomplete correction and cause the partial injection of structured noise into the "corrected" image. For all digital detector systems, if variations caused by structured noise or other artifacts are noted at any time (during inspections, on patient images, etc), a flat-field calibration should immediately be performed before further patient imaging. Also, calibration should be implemented after any repairs of the system directly related to

digital detector operation. With digital systems, quantitative methods to ascertain the quality of the acquisition processing and the removal of static and structured noise should be straightforward by uniformly exposing the detector and analyzing the noise properties of the resultant image using methods such as the SNR and more sophisticated methods such as noise power spectrum analysis, as explained in elsewhere in this article.

The final preprocessing step before releasing the data to an image workstation involves signal scaling and data transformation. Signal scaling is a method to identify pertinent image data within the exposed area of the 2-D digital matrix. Most often, this is performed by analyzing the data histogram, which is a frequency distribution of the digital values in the image. The wide dynamic range of the detector response is sensitive to unimportant information caused by high x-ray attenuation (eg, collimated areas) and low x-ray attenuation (eg, uncollimated areas), signals that do not contribute to the image. The histogram distribution depicts the minimum and the maximum useful areas related to breast information, as well as the nonuseful parts. Once the useful range is identified, the image data contained within that range is converted into an output range with linear or nonlinear (eg, logarithmic) transforms, typically into 12-bit (4,096 gray levels) or 10-bit (1,024 gray levels) depth. This transform produces the unenhanced raw breast image (also referred to in Digital Imaging and Communications in Medicine terminology as the for-processing image) that is sent to the image workstation for contrast and spatial resolution enhancement and processing [26].

Detectors used for digital mammography can also have a certain number of dead dels. Manufacturers can mask the appearance of these by assigning a signal value to the corresponding displayed pixel that is based on the values of adjacent dels (eg, a simple average). If these dead dels are single, isolated from one another, and not too numerous, the significance of these to image quality is likely to be low. On the other hand, if there are patches or lines of such defective elements, image quality could be degraded. Although the cost of producing a perfect detector with fewer than 1 such del per 5 to 10 million would be prohibitive, manufacturers should provide a map of dead dels for each detector on installation.

In addition to noise sources associated with the detector, there will be some level of granularity associated either with the soft-copy display device or with the film used to print the hard-copy digital images. For example, different phosphor materials used in display monitors will vary in granularity and can affect the displayed noise power spectrum and SDNR [27].

Other sources of unwanted image detail are artifacts that appear in an image and are unrelated to anatomic structures within the breast. Artifacts have 2 detrimental

effects on mammographic quality: they can mask the detection or impair the characterization of lesions by adding clutter [28] or noise to the image, and they can simulate lesions that do not exist. Artifacts can be caused by the x-ray source, beam filter, compression device, breast support table, grid, and screen. These have been well documented in the literature [29,30], and their evaluation should be part of any QC program for mammography. In digital mammography, additional artifacts can be caused by nonuniformities in the detector response over the image area. These may be a result of improper flat-fielding, errors in scanning, or mismatches in stitching together subimages from detectors that contain multiple modules. With good design and proper maintenance and system calibration, it should be possible to control or eliminate these artifacts.

DEVELOPMENT OF A HARMONIZED FULL-FIELD DIGITAL MAMMOGRAPHY QC MANUAL

All facilities striving to perform high-quality digital mammography must have effective QC programs specifically designed for digital mammography. Currently, the US Food and Drug Administration's (FDA) mammography regulations require facilities to follow quality assurance programs that are substantially the same as the quality assurance programs recommended by the image receptor manufacturers. Consequently, each digital equipment manufacturer provides its users with QC procedures specific to its equipment. At the time of this writing, there are 5 models of digital equipment approved by the FDA for use in mammography from 4 different manufacturers, each with its own set of QC procedures. The required tests, frequencies, and performance criteria are significantly different across all manufacturers and models. This nonuniformity is not necessarily based on objective evidence. Furthermore, the manufacturers constantly revise their QC manuals as they upgrade software and gain more experience with their own tests and performance criteria. This ever-changing nonuniformity complicates QC testing and evaluation for mammography technologists and medical physicist and results in severe inefficiencies as the use of digital mammography grows and more facilities install multiple units from different manufacturers.

Considerable experience in testing the performance of digital mammography systems was gained in the course of the ACR Imaging Network[®] Digital Mammographic Imaging Screening Trial, and lessons learned from the trial have been documented [31,32]. This QC experience is being used by the ACR's Subcommittee on Digital Mammography in the development of a harmonized digital mammography QC manual. The goal of this manual

is to provide users with a practical and clinically relevant set of QC procedures that may be performed on any digital system. This endeavor is being modeled on the highly successful 1999 ACR *Mammography Quality Control Manual* (which is used by technologists and medical physicists from almost 9,000 mammography facilities across the United States) to best use that existing broad knowledge base. The manual will be divided into radiologic technologists' tests, with frequencies ranging from daily to semiannually, and medical physicists' tests, which should be performed annually or when significant changes or repairs have been made to the system. A draft version of the manual will be provided to digital equipment manufacturers and the FDA for review and comment before publication, with the anticipation that the FDA will eventually incorporate critical elements of the final version into its regulations. This will be critical to ensure that facilities meet FDA regulations as they use these tests and criteria. We withhold any in-depth discussion of QC in this paper and defer to the pending harmonized ACR full-field digital mammography quality control manual when it becomes available.

REFERENCES

- International Commission on Radiation Units and Measurements. ICRU report 54, medical imaging—the assessment of image quality. Bethesda, Md: International Commission on Radiation Units and Measurements; 1996.
- Green D, Swets J. Signal detection theory and psychophysics. New York, NY: John Wiley; 1966.
- Metz CE. Basic principles of ROC analysis. *Semin Nucl Med* 1978;8:283-98.
- Fukunaga K. Introduction to statistical pattern recognition. New York, NY: Academic Press; 1972.
- Fujita H, Tsai D, Itoh T, et al. A simple method for determining the modulation transfer function in digital radiography. *IEEE Trans Med Imag* 1992;11:34-9.
- Williams M, Mangiafico PA, Simoni P. Noise power spectra of images from digital mammography detectors. *Med Phys* 1999;26:1279-93.
- Yaffe MJ, Jong R. Image quality in digital mammography. In: Samei E, Flynn M, editors. *Advances in digital radiography: categorical course in diagnostic radiology physics*. Oak Brook Ill: Radiological Society of North America; 2003. p 123-42.
- Swets J, Pickett R. Evaluation of diagnostic systems—methods from signal detection theory. San Diego Calif: Academic Press; 1982.
- Vyborny CJ, Schmidt RA. Technical image quality and the visibility of mammographic detail. In: Haus AG, Yaffe MJ, editors. *A categorical course in physics: technical aspects of breast imaging*, 3rd ed. Oak Brook Ill: Radiological Society of North America; 1994. p 103-10.
- Rossmann K. Point spread-function, line spread-function, and modulation transfer function: tools for the study of imaging systems. *Radiology* 1969;93:257-72.
- Samei E, Flynn MJ, Reimann DA. A method for measuring the presampled MTF of digital radiographic systems using an edge test device. *Med Phys* 1998;25:102-13.
- Pisano ED, Gatsonis C, Hendrick E, et al. Diagnostic performance of digital versus film mammography for breast-cancer screening. *N Engl J Med* 2005;353:1773-83.
- Barnes GT, Brezovich IA. Contrast: effect of scattered radiation. In: Logan WW, editor. *Breast carcinoma: the radiologist's expanded role*. New York, NY: John Wiley; 1977.
- Barnes GT, Brezovich IA. The intensity of scattered radiation in mammography. *Radiology* 1978;126:243-7.
- Wagner AJ. Contrast and grid performance in mammography. In: Barnes GT, Frey GD, editors. *Screen film mammography: imaging considerations and medical physics responsibilities*. Madison, Wis: Medical Physics Publishing; 1991. p 115-34.
- Yaffe MJ, Hendrick RE, Feig SA, Rothenberg LN, Och J, Gagne R. Recommended specifications for new mammography equipment: report of the ACR-CDC focus group on mammography equipment. *Radiology* 1995;197:19-26.
- Barnes GT. Radiographic mottle: a comprehensive theory. *Med Phys* 1982;9:656-67.
- Swank RK. Absorption and noise in x-ray phosphors. *J Appl Phys* 1973;44:4199-203.
- Nishikawa RM, Yaffe MJ. Signal-to-noise properties of mammographic film screen systems. *Med Phys* 1985;12:32-9.
- Rossmann K. Effect of quantum mottle and modulation transfer on the measurement of radiographic image quality. In: Moseley RD, Rust JH, editors. *Diagnostic radiologic instrumentation*. Springfield, Ill: Thomas; 1965. p 350.
- Bunch PC, Huff KE, Van Metter R. Analysis of the detective quantum efficiency of a radiographic screen-film combination. *J Optical Soc Am* 1987;4:902-9.
- Wagner RF. Physical performance of diagnostic imaging modalities. *Acad Radiol* 1999;6(suppl 1):S69-71.
- Yaffe MJ, Nishikawa RM. X-ray imaging concepts: noise, SNR and DQE. In: Seibert JA, Barnes GT, Gould RG, editors. *Specification, acceptance testing and quality control of diagnostic x-ray imaging equipment*. Woodbury, NY: American Institute of Physics; 1994. p 109-44.
- Critten JP, Emde KA, Mawdsley GE, Yaffe MJ. Digital mammography image correction and evaluation. In: Doi K, Giger ML, Nishikawa RM, Schmidt RA, editors. *Digital mammography '96. Excerpta Medica International Congress Series* 1996;1119:455.
- Yorker JG, Jeromin LS, Lee DLY, et al. Characterization of a full field digital mammography detector based on direct conversion in selenium. In: Antonuk L, Yaffe M, editors. *Medical imaging 2002: physics of medical imaging, proceedings SPIE 2002;4682:21-9*.
- Seibert JA. Digital radiographic image presentation: pre-processing methods. In: Samei E, Flynn M, editors. *Advances in digital radiography: categorical course in diagnostic radiology physics*. Oak Brook, Ill: Radiological Society of North America; 2003.
- Krupinski E, Johnson J, Roehrig H, et al. Using observer models to predict softcopy performance with digital mammography. In: Peitgen H-O, editor. *Proceedings of the 6th International Workshop on Digital Mammography*. Berlin, Germany: Springer-Verlag; 2003. p 463-7.
- Kundel HL, Revesz G. Lesion conspicuity, structured noise, and film reader error. *Am J Roentgenol* 1976;126:1233-8.
- Haus AG, Jaskulski SM. *The basics of film processing in medical imaging*. Madison, Wis: Medical Physics Publishing; 1997.
- American College of Radiology. *Mammography quality control manual for radiologists, medical physicists, and technologists*. Reston, Va: American College of Radiology; 1999.
- Bloomquist AK, Yaffe MJ, Pisano ED, et al. Quality control for digital mammography in the ACRIN DMIST trial—part I. *Med Phys*. In press.
- Yaffe MJ, Bloomquist A, Mawdsley GE, et al. Quality control for digital mammography—part II: recommendations from the ACRIN DMIST trial. *Med Phys*. In press.